CO12-1 Analysis of Heavy Metal Elements in Chinese Medicine

E. Furuta, S.Ishihara, R.Okumura[1] and Y. Iinuma[1]

Ochanomizu University

[1]Research Reactor Institute, Kyoto University

INTRODUCTION: Chinese medicine has been used for a long time among many countries because of its safety image. However, some of them are famous to include of some toxics elements like arsenic (As). Recently, it is easy to purchase Chinese medicine and herbs from abroad though the Internet. On the other hand, each country has each regulation for ingredients of medicines. The purpose of this study was to show the ingredient of Chinese medicine and herbs.

EXPERIMENTS: Samples used in this study are shown in Table 1. The sample was grinded into powders

Table 1 Sample information

	Name	Purchased at	Kinds	Specialty
1	Chinese Medicine	Shanghai /Chaina	12	Doctor's prescription
2			8	Internet from Tokyo
3		Seoul/Koria	11	Market at Seoul
4		Tokyo/Japan	35	Market at Tokyo
5	Herb	Hanoi/Vietnam	47	Market at Hanoi

with an agate mortar and enclosed each in a double polyethylene bag by measuring their weight. The standard samples used were JA-2 and JR-2 of rock standard, and 50 ppm of As, mercury (Hg), antimony (Sb), cobalt (Co) and chromium (Cr) of atomic absorption reagents (Wako) were used applying to 5 filter papers (Advantec 5A). The samples and the standards were put in capsules and irradiated 1MW × 30 min at KUR. After cooling among 5 to 10 days, the capsules were opened, and then the gamma-rays of medium and long half life radionuclides were measured.

RESULTS: Table 2 shows the amounts of remarkable elements in some parts of No.1 samples. Two samples

Table 2 Concentration of heavy metal elements in some Chinese medicine ppm

Name	Cr	Co	As	Hg	Sb
牛黄解毒片	<47	<3.7	83000 ±2000	—	250 ±4.3
六神丸	<141	<7.8	74000 ±15000	74000 ±15000	330 ±50
胃气疼片	62±4.9	1.7±0.18	12±2.6	2.0±1.1	0.40 ±0.34
麻仁丸	<0.49	0.29	<1.0	44±3.3	0.22

showed high concentration of As and Hg. On the other hand, 37 herbal samples (No.5) included low concentration of Hg, 0.6 to 3 ppm. The No.2 samples and the No.3 samples included less amounts of heavy metal elements. Almost all the Japanese samples (No.4) included no heavy metal elements.

DISCUSSION: About 2 of the above, the *Niuhuang Jiedu Pian* (牛黄解毒片) shows As inclusion as the ingredient, however, the *Liushen Wan* (六神丸) expresses no ingredients with its products. These two medicines also included relatively high concentration of Sb. It suggested that As was derived from minerals of Realger because Realger; As_4S_4 exists with Stibnite; Sb_2S_3. So, As included in the *Liushen Wan* (六神丸) came from Realger.

In the terms of Hg, there is one possibility that the concentration of the element was influenced by environmental pollution, soil and air of the area where the plants grew.

CONCLUSION: Chinese medicine is taken for a long time because of its safe image, however, some indications were not enough to show the ingredients of toxics elements. So, personal import of medicines from different medical regulated countries needs caution.

採択課題番号 25004 漢方薬剤に含まれる重金属元素の分析 共同通常

（お茶の水女子大学）古田悦子、石原祥子 （京大・原子炉）奥村良、飯沼勇人

CO12-2 Terahertz Absorption Sepctrum of Carbohydrates Including Water

M. Kawase and T. Tahakashi[1]

Faculty of Bioscience, Nagahama Institute of Bio-science and Tecnology
[1]Research Reactor Institute, Kyoto University

INTRODUCTION: Various applications of terahertz (THz) electromagnetic waves have been reported in many fields, such as medical diagnosis, pharmaceutical analysis, and security enhancement. Absorption spectra in the THz range are very sensitive to differences in the crystal structure [1], and are applied to study the polymorphs of medicines [2]. THz spectra are also sensitive to the states of assembled molecules. Cellulose attracts attention as eco-material. It is also well known that cellulose interact with various chemicals, such as carbohydrates, under existence of water. In this study, observation of interaction between cellulose and carbohydrates under existence of water is tried by using coherent THz wave. Water is known to interfere with THz measurement, and development of THz measurement method is required for water-containing materials to enlarge the applied field of THz. This attempt is a part of the development of THz measurement system for water-containing materials.

EXPERIMENTS: Coherent THz wave was obtained from the transition radiation generated by L-band linear accelerator in Kyoto University Research Reactor Institute. The absorption spectra were measured as time-domain signal by the composite type liquid-helium-cooled silicon bolometers after through Martin-Puplett type interferometer and sample. Sample was prepared as follows: carbohydrate solution was dropped on cellulose membrane. Cellulose membrane was used as reference sample. In the measurement of powder sample, air was reference. By Fourier transforming the time-domain signal, the amplitude spectra were obtained [3]. All chemicals were obtained from commercial sources.

RESULTS: Arabinose, galactose, glucose, fructose, fucose and xylose were used. In THz spectra of arabinose and glactose, the effect of water was clearly observed. The obtained spectra were shown in Figs. 1 and 2. In both spectra, absorption modes disappeared by interaction with cellulose from 5 to 17 cm^{-1}. This result suggests that such disappearance is occurred by interaction between cellulose and carbohydrates. Moreover, absorption modes also disappeared over 17 cm^{-1} for dried samples.

In arabinose sample, the same shape was observed over 17 cm^{-1} in both powder and wet samples. However, in dried sample, such absorption disappeared. These results suggest that vibration or rotation over 17 cm^{-1} of arabinose is restrained by interaction with cellulose without water. Under existence of water, there is not such restraint. The same phenomena is considered to happen in galactose. In future study, we will try to develop method for measurement of solution, and clarify the role of water in interaction between cellulose and carbohydrates.

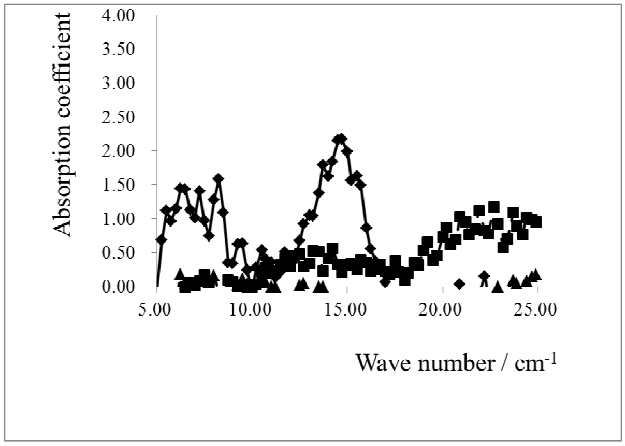

Fig. 1 THz absorption spectra of galactose powder (powder sample, ◆), galactose on cellulose (wet sample, ■) and galactose on cellulose (dried sample, ▲)

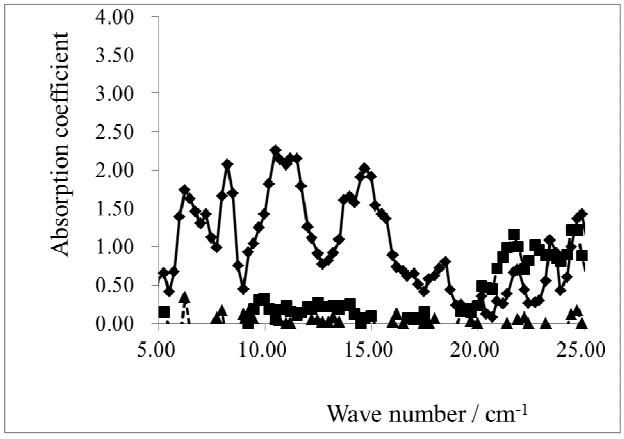

Fig. 2 THz absorption spectra of arabinose (powder sample, ◆), arabinose on cellulose (wet sample, ■) and arabinose on cellulose (dried sample, ▲)

REFERENCES:

[1] Y. S. Lee, "*Principles of Terahertz Science and Tech nologyy*" Springer, 2009.

[2] P. F. Taday, I. V. Bradley, D. D. Arnone, and M. Pepper,*J. Pharm. Sci*., **92** (2003) 831-838.

[3] T. Takahashi, T. Matsuyama, K. Kobayashi, and Y. Fujita, *Rev. Sci. Instrum.*, **69**(1998) 3770-3775.

採択課題番号 25006　含水および水溶液系でのコヒーレントテラヘルツ吸収測定法の開発　共同通常
（長浜バイオ大）川瀬雅也（京大・原子炉）高橋俊晴

CO12-3 Neutron Activation Analysis for Hafnium in Hafnium Oxide Thin Films

T. Takatsuka and K. Hirata.

National Metrology Institute of Japan, National Institute of Advanced Industrial Science and Technology

INTRODUCTION: Hafnium oxide (high-k) dielectric films are being introduced into silicon-based semiconductor devices in order to achieve higher electronic performance. The front-end processes require the thin dielectric films well-controlled in thickness for gate stacks. Thickness of the dielectric films should be controlled in 4 % process range, according to the international technology roadmap for semiconductors 2011[1]. Certified reference material NMIJ-CRM 5605-a was developed in 2012 [2], which is applicable to quantify the film thickness with small uncertainties. This study aims to confirm the stability of hafnium quantity in thin hafnium oxide films by neutron activation analysis, in order to keep the reliability of the reference material.

EXPERIMENTS: For the certified reference material, hafnium oxide films were deposited on 4-inch Si wafers by magnetron sputtering method and were diced into 10 × 10 mm^2 pieces. Several pieces were picked-up for measurements.

Hafnium amounts were evaluated by INAA. For the production of standards to calibrate hafnium amounts, a natural standard solution was prepared by diluting SRM 3122 (commercially available from NIST) gravimetrically. In addition, a standard solution for internal standard was prepared by diluting JCSS antimony standard solution gravimetrically. A portion of the antimony solution was dropped from a polyethylene pipette onto a cleaned filter paper on the cleaned specimen. Portions of mixed solution (hafnium and antimony standards) were dropped onto cleaned filter papers for the standards. All specimens and standards were heat-sealed in individual clean poly-ethylene envelopes and stacked in a poly-ethylene irradiation container. The neutron irradiation was performed for 4 hours at 1 MW in research reactor KUR of Research Reactor Institute, Kyoto University. Gamma-ray activity of each specimen and standard was measured by a high-purity germanium detector (CANBERRA).

RESULTS: Figure 1 shows a gamma ray spectrum obtained from the specimen of hafnium oxide film with antimony internal standard solution. The peaks at around 482 keV from ^{181}Hf and 603 keV from ^{124}Sb were focused to determine hafnium amount in the oxide film. The counts in each peak were integrated for every specimen and standard, and then the intensities after the decay correction [3] were used to calculate relative intensities (^{181}Hf cps) / (^{124}Sb cps/ ng). The hafnium content in the specimen is estimated to be 3.58 µg from the calibration curve shown in Fig. 2. Considering the surface area of the hafnium oxide film is 97.1 mm^2, the resulting hafnium content is 3.69 µg / cm^2 with a relative standard uncertainty of 0.92 %. This result agrees with the certified value of the certified reference material, considering uncertainties.

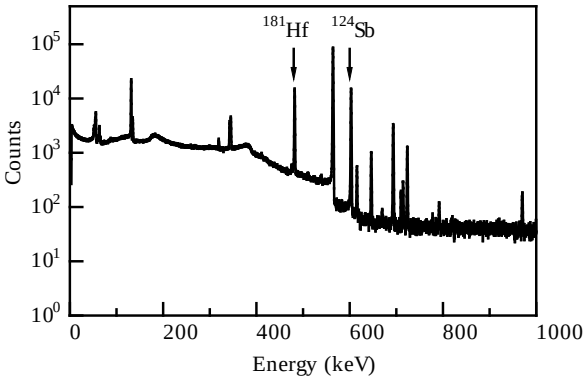

Fig. 1. Gamma ray spectrum from the hafnium oxide film with antimony standard solution.

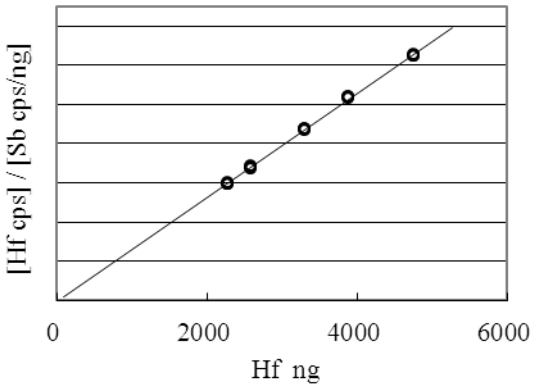

Fig. 2. Calibration curve obtained with the standards.

REFERENCES:

[1] The International Technology Roadmap for Semiconductors 2011.
[2] KURRI Progress Report 2012.
[3] G.Gilmore and J. D. Hemingway, Practical gamma-ray spectrometry (John Wiley & Sons, Chichester, 1995.

採択課題番号25020　中性子放射化分析によるハフニウム酸化膜中ハフニウムの定量　一般通常
（産総研・計測標準）高塚登志子、平田浩一

CO12-4 Basic Research on Radiation Tests Suitable for Nano-Satellites

T. Tomioka, H. Masui, M. Cho and K. Takamiya[1]

Kyushu Institute of Technology
[1]Research Reactor Institute, Kyoto University

INTRODUCTION: In recent years, many nano-satellites are being developed in universities and private enterprises, and characteristics of nano-satellites include low-cost development. Satellites should undergo radiation tests before launch. Conventional radiation tests require an accelerator. However, this cost is too high for nano-satellites. So, we are focusing on Californium252.

EXPERIMENTS: The purpose of this test is to cause SEL (Single-Event-Latchup) using Californium252. SEL is the phenomenon that generates over-current in the IC. The bombardment target is the microprocessor H8/36057. The plastic package was removed to enhance radiation particle penetration (Fig.1).

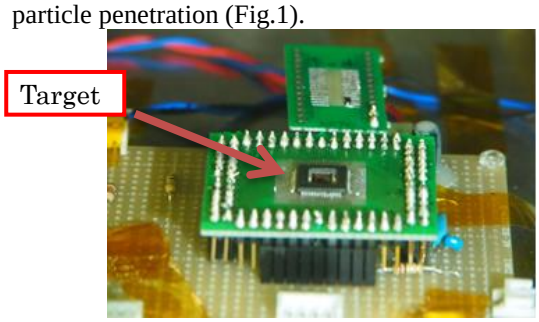

Fig. 1. Irradiation targets

The experimental schematic is illustrated in Fig. 2. We monitored the current consumption using this system.

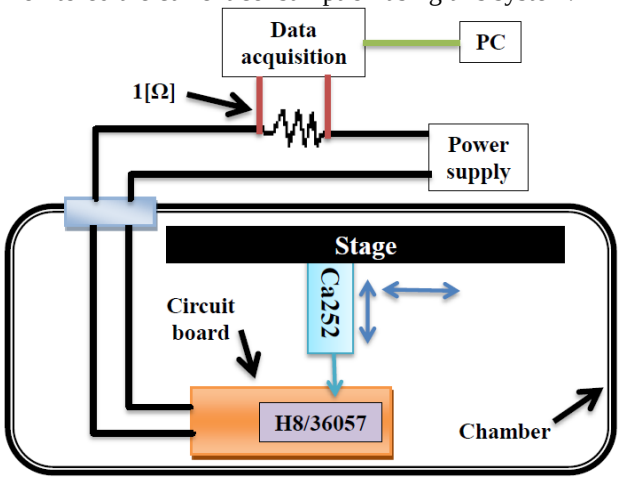

Fig. 2. Experimental schematic

RESULTS: While the target was irradiated, we detected malfunction of the H8 processors. Fig.3 shows the current consumption of the circuit boards. First, the radiation source was placed over H8 at 0 sec. During the section (1), the experimental board was working normally. In section (2), malfunction of H8 occurred at 9 sec and the current was increased to 175 mA. At (3), the H8 processors were rebooted and returned to normal mode.

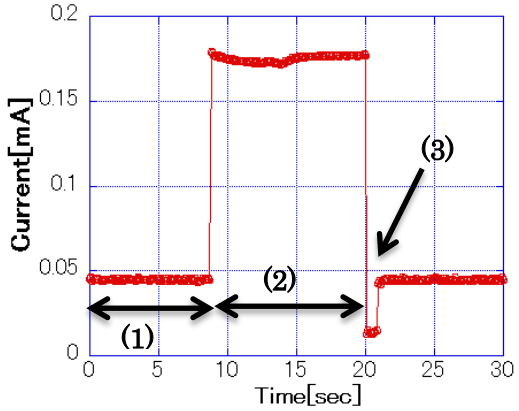

Fig. 3. Consumption current of H8/36057

We conducted this test at four distances (between target and radiation source) to change the flux. We tried 10 tests at each distance. During each test, we measured the time until SEL occurred. Table 1 shows the minimum, maximum and average time of each 10 tests until SEL occurred at each distance.

Table.1 Time elapsed until SEL occurred

	Time[sec]			
	1[cm]	2[cm]	2.5[cm]	3[cm]
Min	3	6	7	27
Max	34	229	204	299
Ave	17	77	61	99

The average time of 2cm was longer than that of 2.5cm, which still needs investigation.

Next, we calculated the SEL cross-section according to the following equation.

$$cross-section = \frac{1}{Ave.time \times flux}[cm^2/ions]$$

Table 2 shows the cross-section at each distance.

Table.2 Flux and Device surface

distance [cm]	flux to surface [ions/sec/cm^2]	cross-section [cm^2/ions]
1	17.5	0.0035
2	4.39	0.0030
2.5	2.81	0.0059
3	1.95	0.0052

The SEL cross-section is between 0.0030 and 0.0059cm^2/ions within a factor of two variation. For H8/36057, we have the on-orbit data of SEL occurrence based on the flight results of HORYU-Ⅱ. It is as short as 18 days at 680km Polar Earth Orbit [1]. Using these numbers as references, we can obtain the first-order estimate of the SEL probability in orbit by comparing the SEL cross-section to that of H8/36057.

REFERENCES:

[1] Y. Okumura *et al*, 64th International Astronautical Congress, IAC-13-6B, 2013

採択課題番号 25025　　カリフォルニウム線源を使用した衛星搭載用オンボードコンピュータに発生するシングルイベントの模擬試験および試験方法の確立　　共同通常

（九工大・先端）冨岡　孝裕、増井　博一、趙　孟佑（京大・原子炉）高宮　幸一

CO12-5 Photon Activation Analysis of Fluorine with Bremsstrahlung at the KURRI-Linac

T. Kubota and T. Ohta[1]

Research Reactor Institute, Kyoto University
[1]Graduate School of Engineering, Hokkaido University

INTRODUCTION: Bremsstrahlung, photon, generated through the bombardment of high-energy electron to heavy metal such as tantalum and platinum can be used for isotope production and activation analysis. In such isotope production, unlike nuclear reactor, neutron deficient radionuclides can be produced [1-2]. At the KURRI-Linac many useful radionuclides are produced; however, sample handling is conducted inside high dose area, Target room. We built a new sample transport system, where samples can be transported between inside and outside the Target room through an experimental hole, in order to suppress external exposure as well as to produce short half life radionuclides. We report the measurement results of irradiated standard silicate samples for observation of (γ, n) and (γ, p) reaction.

EXPERIMENTS: Bremsstrahlung was generated through irradiation of high-energy electron beam of 30 MeV to thin platinum sheets. Because some fraction of the electron beam penetrated the sheets, in order to eliminate such electron beam and to avoid undesirable sample heating, a graphite block was placed between the sheets and a sample. Irradiation samples were prepared as follows: a membrane filter was saturated with silicate standard solution, analytical grade, and sealed into a plastic bag, which was packed with aluminum foil. The sample was placed at the irradiation field by entering the Target Room; however, the sample irradiated was withdrew by pulling on string connected to the sample transport vessel without entering the Target Room. The sample was irradiated for 20 minutes and after cooling down for 57 minutes the resulting radioactivity was measured by gamma spectrometry.

RESULTS: Figure 1 shows a result of radioactivity measurement. The peaks of 511 keV and 1022 keV were ascribed to β^+ radionuclides generated and their sum peak due to high radioactivity, respectively. In contrast, the concentration of ^{28}Al (1.779 MeV) and ^{29}Al (1.273 MeV) was below the detection limit, which suggests that (γ, p) reaction of Si is negligible. Fig 2 shows the change of total count of gamma spectrometry measured for 5 minutes. This decrease can be explained by two radionuclides, i.e. ^{18}F (109.8 min) and ^{34}Cl (32 min). ^{18}F and ^{34}Cl were generated through (γ, n) reaction of fluorine dissolved in the silicate standard solution and of chlorine, i.e. NaCl, from contamination in handling, respectively. Activation analysis using neutron deficient radionuclide with a short half life can be conducted at the KURRI-Linac.

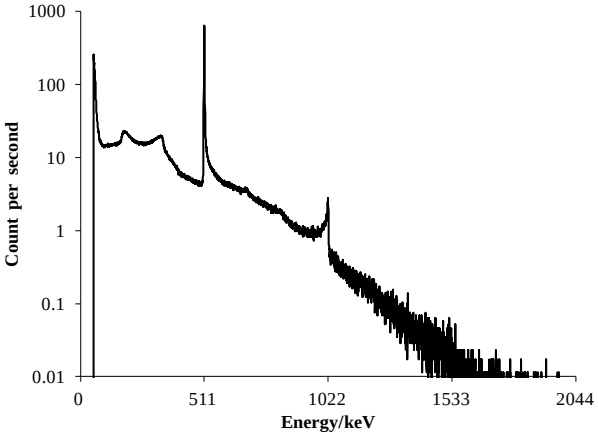

Fig. 1. Gamma spectrometry of irradiated standard silicate sample

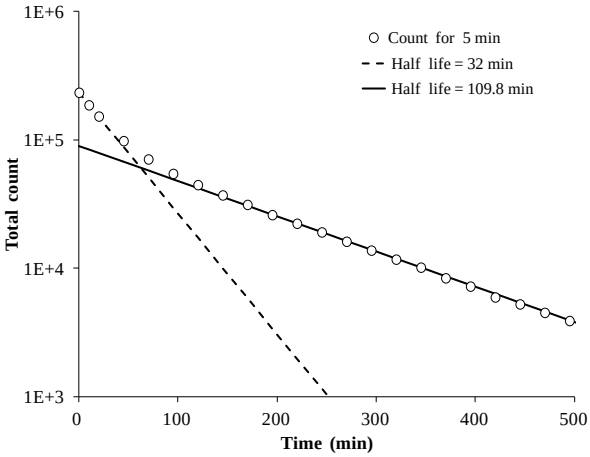

Fig. 2. Change of total count for five minutes

REFERENCES:

[1] T. Fujii *et al.*, J. Radioanal. Nucl. Chem, **262** (2004) 551-554
[2] T. Kubota *et al.*, Recent Advances in Actinide Science Ed: I. May, R. Alvares and N. Bryan RSC Publishing (2006) pp. 68-70

CO12-6 Mössbauer Microspectrometer Using MCX and Estimation of γ-ray Focus Size

K. Shinoda and Y. Kobayashi[1]

Department of Geosciences,
Graduate School of Science, Osaka City University
[1]Research Reactor Institute, Kyoto University

INTRODUCTION: In the last KURRI Progress Report 2012, we introduced Mössbauser microspectrometer using a multi-capillary X-ray lense (MCX) to focus γ-ray and its construction. In the last report, we confirmed that Mössbauer spectrum of α-Fe foil with 6 peaks due to magnetic-splitting can be measured with the spectrometer. But beam size of 14.4keV γ-ray at the focus point of MCX was not certainly estimated. This year, we attached X-Y PC-controlled auto mapping stage to the Mössbauer microspectrometer, and scanned a gold pinhole and tungsten edge using auto mapping stage to estimate 14.4keV γ-ray intensity distribution and full width at half maximum (FWHM) of γ-ray focus size. 6KeV FeK X-ray is also emitted from ^{57}Co γ-ray source and focused as 14.4keV. FWHM of 6keV X-ray was also estimated.

EXPERIMENTS and RESULTS: Gold plates with a pinhole of 3 diameters were scanned in 2 dimension. Table 1 shows a summary of pinhole scan. Proportional counter was used for γ-ray detector.

Fig.1 shows 2 dimensional intensity map of γ -ray at the focus using 286μmϕ pinhole. The intensity distribution was fairly isotropic. Fig.2 shows 1 dimensional intensity distribution of 14.4 keV γ-ray by edge scan. Scanning range, step and exposure time per step were 2000μm, 20μm and 700s, respectively. FWHM of 14.4keV was estimated to 400μm. Fig.3 shows a result for 6keV X-ray. FWHM of 6keV was 650μm. FWHM of focus depends on the energy of γ-ray. We will the same experiments using Si-PIN semi-conductor detector, and fix the spot size of focused γ-ray.

PH diameter(μm)	scan range(μm)	step(μm)	measure points	exp. time(s/point)
530	±1000	250	9×9=81	1080
346	±600	150	9×9=81	1080
286	±600	100	13×13=169	1020

Table 1. Summary of pinhole scan

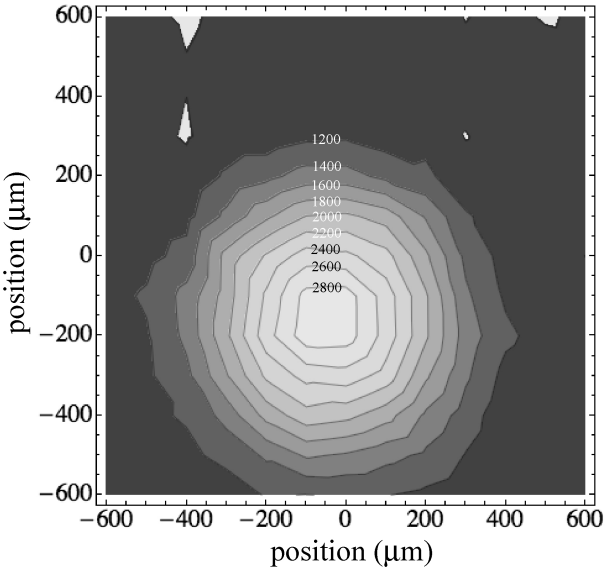

Fig.1 Two dimensional intensity distribution 14.4keV γ-ray at the focus point by pinhole scan.

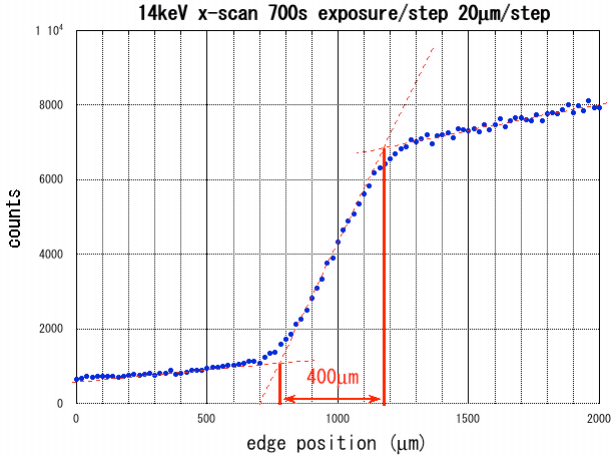

Fig.2 One dimensional intensity distribution 14.4keV g-ray by edge scan at the focus point.

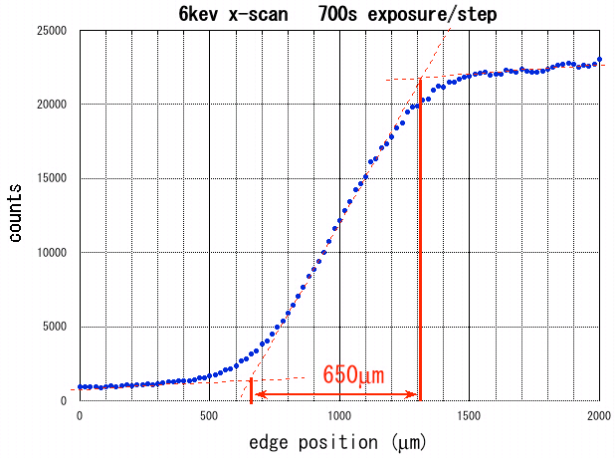

Fig.3 One dimensional intensity distribution of 6keV X-ray by edge scan at the focus point

採択課題番号 25038　マルチキャピラリーX 線レンズを用いた顕微メスバウアー分光法の確立　共同通常
（大阪市大・理）篠田圭司（京大・原子炉）小林康浩

CO12-7 Evaluation of Multiwire-Type Two-Dimensional Neutron Detector with Individual Line Readout

K. Toh, H. Yamagishi[1], K. Soyama, M. Hino[2] and T. Oda[3]

J-PARC center, Japan Atomic Energy Agency
[1]Nippon Advanced Technology
[2]Research Reactor Institute, Kyoto University
[3]Graduate School of Engineering, Kyoto University

INTRODUCTION: We develop a two-dimensional neutron detector system for use in scattering experiments performed at high-intensity pulsed neutron facilities. A short response-time and high spatial resolution can be obtained in our system through the use of an individual line readout method [1,2]. In a high-intensity neutron irradiation facility, there are some difficulties compared to smaller experimental laboratory environments. Examples include the long distance between the sample irradiation area and the data acquisition room, massive and inconvenient neutron shieldings, complicated background noise from complex sample environment, and strong electric fields in the facility. We therefore develop a neutron detector system that uses optical signal transmission devices to ensure that the system can satisfy the challenging requirements of the facility. In the present study, we have performed neutron irradiation experiments using a developed neutron detector system with individual line readout and optical signal transmission.

EXPERIMENTS: In this detector system, we adopt a multiwire-type detector element because of its wide use in neutron scattering experimental facilities and because it has an excellent long-term stability. The developed multiwire element for individual line readout consists of anode wires, first cathode wires (y-axis), and second cathode strips (x-axis). The element has a sensitive area of 128 × 128 mm^2 with a pitch of 1 mm in both x- and y-directions. Gas amplification occurs around the anode wires, and the signal pulses induced at the first and second cathodes are read out individually. The neutron-induced signals are individually amplified, shaped, and discriminated by amplifier-shaper-discriminator application-specific integrated circuits (ASD-ASICs). Digital signals from the ASD-ASIC are transmitted to the position encoders via optical fibers as optical signals that are converted by specially fabricated E/O-O/E converters. Neutron irradiation is performed using a neutron beam line CN3 at the KUR.

RESULTS: Figure1 shows typical neutron-induced pulse shapes at anode wires, a first cathode wire, and a second cathode strip after shaping by the preamplifier in the ASD-ASIC. A signal-pulse peak of neutrons can be clearly observed with a fast temporal response; the full width at half maximum of the response time is 180 ns. The detector system is operated when the KUR is stopped. The elapsed-time dependence of the measured counts after the reactor is stopped is shown in Fig. 2. Here, the time is set to zero when the reactor is stopped, and data from a reactor power monitor is also plotted for comparison. The detector system exhibits a timely response to the reactor power, and it can counts neutron-induced signals over five orders of magnitude.

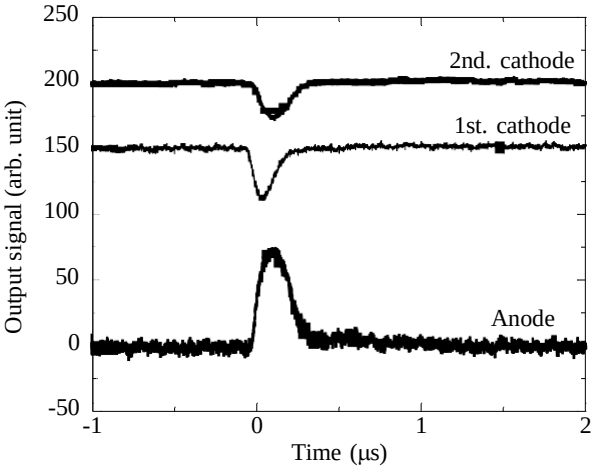

Fig. 1 Neutron-induced analog signal at anode wires, a first cathode line, and a second cathode strip.

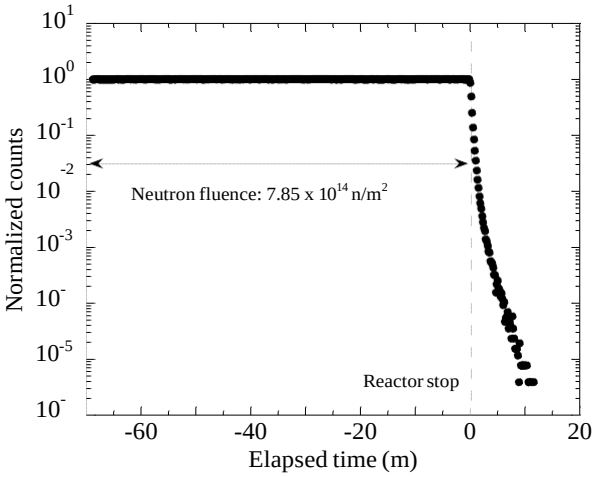

Fig. 2. Elapsed-time dependence of measured signals of developed detector.

REFERENCES:

[1] H. Yamagishi *et al.*, J. Instrum., **6** (2011) C12025.
[2] K. Toh *et al.*, Nucl. Instr. and Meth., **726** (2013) 169-174.

採択課題番号 25042　個別信号読み出し MWPC 二次元中性子検出器の特性評価　　共同通常
（原子力機構）藤　健太郎、曽山　和彦（日本アドバンストテクノロジー）山岸　秀志
（京大・原子炉）日野　正裕（京大院・工）小田　達郎

CO12-8

Precise Determination of Cl in ABS Resin by Instrumental Neutron Activation Analysis Using Internal Standardization

T. Miura, R. Okumura[1], Y. Iinuma[1], S. Sekimoto[1] and K. Takamiya[2]

[1]National Metrology Institute of Japan, AIST
[2]Research Reactor Institute, Kyoto University

INTRODUCTION: National Metrology Institute of Japan is responsible for developing certified reference materials (CRMs) and for establishing the traceability of SI (The International System of Units) on chemical metrology in Japan. To establish SI traceability, the primary method of measurements should be applied to the characterization of the CRMs. Recently, neutron activation analysis (NAA) using comparator standard is recognized as a potential primary ratio method [1]. Despite the potential of NAA as primary ratio method, the evaluation of the measurement uncertainty is required in any analysis. In general, there are three main components of uncertainty in NAA, that is, sample preparation uncertainty, neutron flux homogeneity, and gamma ray measurement uncertainty. Usually, flux monitor is used to correct the neutron flux in-homogeneity. However, although the flux monitor can correct the neutron flux variation using the count rate of the known amount of the monitor nuclide, it does not reflect the neutron flux of the actual sample. The most practical method to eliminate neutron flux in-homogeneity and to improve gamma ray measurement uncertainty is an internal standard method [2]. In this paper, we presented that notable capability of internal standardization in NAA for determination of Cl in acrylonitrile butadiene styrene copolymer (ABS) resin as a candidate CRM.

EXPERIMENTS: The ABS resin candidate CRM was produced by a mixing machine. The calibration solution of Cl was prepared from NMIJ primary standard solutions. The In solution for the internal standard for Cl was prepared from a high purity metal. The calibration solutions contained Cl and In as internal standard. One hundred mg of the ABS resin samples was used for Cl analysis. The In solution was added to the samples before neutron irradiation. The neutron irradiations were performed by KUR (Kyoto University Research Reactor) PN-3(thermal neutron flux: 4.6 x 10^{12} $cm^{-2}s^{-1}$) for 5 min. The γ ray measurement system consisted of a Canberra GC4070-7500 Ge detector and a Laboratory Equipment Corporation MCA600.

RESULTS: It was found that the ^{116m}In sensitivity (cps/μg) varied according to each irradiation capsule (n=9). The relative standard deviation of the ^{116m}In sensitivity (cps/μg) was 11 %. The uncertainty related to the neutron flux homogeneity significantly contributes to the overall uncertainty, if an internal standard is not applied. The amount of Cl in the ABS resin sample was determined by bracketing calibration method using internal standardization.

The analytical results of Cl in BCR-681 certified reference material of polyethylene resin by proposed method were in excellent agreement with the certified value. The analytical results of Cl in ABS resin sample by proposed method was 321 mg/kg±5.7 mg/kg (n=9). The relative expanded uncertainty (*k*=2) was 1.8 %.

REFERENCES:

[1] R.Greenberg, P. Bode, E. De Nardi Fernandes, *Spectrochim. Acta B*, 66 (2011) 193-241.
[2] T. Miura, K.Chiba, T. Kuroiwa, T. Narukawa, A.Hioki, H. Matsue, *Talanta*, 82 (2010) 1143-1148.

採択課題番号 25049 内標準法を併用した中性子放射化分析法の高精度化に関する研究　共同通常
（産総研・計測標準）三浦勉（京大・原子炉）関本俊、奥村良、飯沼勇人、高宮幸一

CO12-9 Structural Analysis of Oil-Compatible Concentrated Polymer Brushes by Means of Neutron Reflectometry

T. Hirayama, N. Hanamoto[1], C. Araki[1], N. Yamashita[1], T. Matsuoka[1], M. Hino[2] and T. Oda[2]

Dept. of Mechanical Engineering, Doshisha University
[1]Dept. of Mechanical Engineering, Doshisha University
[2]Research Reactor Institute, Kyoto University

INTRODUCTION: 'Polymer brush' is a general term for grafted polymer chains onto material surfaces physically or chemically, and its features depend on the grafting density. Recent development of polymerization technique enabled to make polymer brushes with high grafting density and uniform length, which are called 'concentrated polymer brushes'. The concentrated polymer brushes have different features from semi-dilute polymer brushes, such as higher swelling performance in good solvent, higher compression modulus of elasticity, unique size exclusion effect, and excellent tribological properties etc [1]. Focusing on the tribological properties, some kinds of polymer brushes showing ultra-low friction coefficients under lubrication, less than 0.01, were already found. However, it is still unclear why such polymer brushes could contribute to attain super low friction sliding. Particularly, the studies on oil-compatible concentrated polymer brushes for application to sliding surfaces in machines are not so many, while many studies on hydrophilic polymer brushes mimicking living body are easily found.

In this study, neutron reflectometry was used as methods to investigate the polymer structure in solvents and friction properties of polymer brushes. Neutron reflectometry is possible to show the film thickness, density and composition in the depth direction of the thin polymer film in solvents. The relationship between the polymer structure in solvents and its friction properties was investigated and discussed.

EXPERIMENTS: For Neutron reflectometry, silicon blocks with concentrated polymer brushes grafted onto the surface were prepared. Three kinds of polymer brushes were used for the study; PMMA, PLMA, and PCHMA, and three kinds of solvents were used; deuterated water, deuterated toluene, and deuterated hexadecane.

The reflectivity profiles of PLMA and PCHMA brushes in hexadecane are presented in Fig. 1. The reflectivity profiles were obtained by the neutron reflectometry SOFIA in J-PARC MLF facility. The swelling ratios (= swelling chain length / theoretical full chain length) of PLMA and PCHMA brushes in hexadecane were 0.48 and 0.23, respectively.

We performed the tribological tests for the PLMA and PCHMA brushes in base oil by using nanotribometer (CSM Instruments). The friction coefficient of PLMA brush was lower than 0.01, but that of the PCHMA brush was comparatively high, over 0.1. It means that the swelling ratio of brushes in solvent is quite important, and the swelling state of brushes in good solvent is necessary to achieve low friction properties.

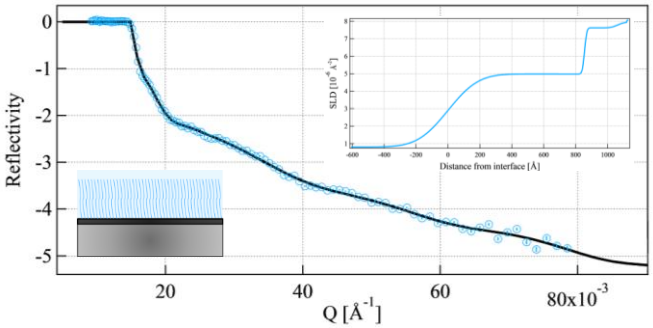

(a) PLMA brush

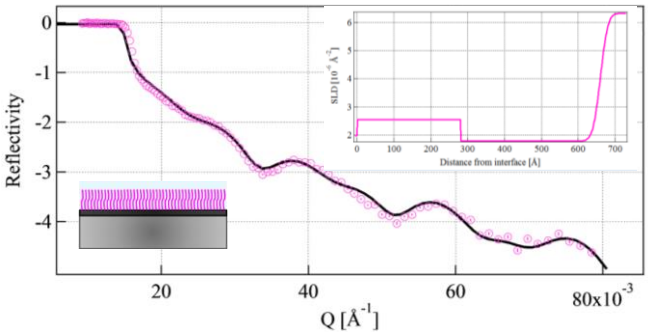

(b) PCHMA brush

Fig. 1. Neutron reflectivity profiles of two kinds of brushes in deuterated hexadecane

CONCLUSIONS: The obtained conclusions from all experiments are shown as follow.
(1) Neutron reflectometry was suitable for in-situ structural analysis for oil-compatible concentrated polymer brushes in solvent.
(2) The total thickness of three kinds of polymer brushes, PMMA, PLMA, and PCHMA, in deuterated toluene was approximately 135 nm, 115 nm, and 56 nm, respectively, and the swelling ratio of each brush was about 0.66, 0.53, 0.57, respectively.
(3) The PLMA brush was swollen in hexadecane, but the PCHMA brush was not swollen in hexadecane because the hexadecane is poor solvent for PCHMA brush. The friction coefficient of PLMA brush in a base oil was lower than 0.01, while that of PCHMA in the base oil was comparatively high, over 0.1.

REFERENCES:
[1] A. Nomura *et al.*, Macromolecules, Vol. 44, No. 12 (2011) pp. 5013-5019.

採択課題番号 25060　中性子反射率法による親油性濃厚ポリマーブラシの構造解析　共同通常
（同志社・理工）平山朋子、花本直哉、荒木千尋、山下直輝、松岡敬
（京大・原子炉）日野正裕、小田達郎

CO12-10 Mössbauer Studies on Reversible O-O Bond Scission of Peroxodiiron(III) to High-Spin Oxodiiron (IV) with a BPG_2E Ligand

M. Kodera, T. Tuji and S. Kitao[1]

Department of Molecular Chemistry and Biochemistry, Doshisha University
[1]Research Reactor Institute, Kyoto University

INTRODUCTION: Peroxodiiron(III) and high-spin oxodiiron(IV) are key intermediates in dioxygen activation of O_2-activating non-heme diiron enzymes,[1] soluble methane monooxygegenase (sMMO), toluene/*o*-xylene monooxygenase (ToMO), toluene monooxygenase (TMO), deoxyhypusine hydroxylase (DOHH). The diiron centers exist at a common carboxylate-rich site, but the reactivity and spectral features are different from one another. The carboxylate donor may control reactivity of the key intermediates, but the roles in the dioxygen activation and the substrate oxidation have not been clarified yet.

Recently, we have shown that efficient catalytic epoxidation with H_2O_2[2] and spectroscopic characterization of peroxodiiron(III) and high-spin oxodiiron(IV) generated via reversible O-O bond scission[3] are attained using μ-oxodiaquadiiron(III) complex with 6-hpa $[Fe_2(\mu\text{-}O)(H_2O)_2(6\text{-hpa})](ClO_4)_4$ (**1**), where 6-hpa is 1,2-bis[2-[bis(2-pyridylmethyl)aminomethyl]-6-pyridyl]ethane. A similar dinucleating ligand where the pyridyl groups of 6-hpa are substituted with the carboxylate groups may be useful for examining roles of carboxylate-rich coordination environment of O_2-activating non-heme diiron enzymes. So, we synthesized a new carboxylate-containing dinucleating ligand, 1,2-bis[2-(*N*-2-pyrid-ylmethyl-*N*-glycinylmethyl)-6-pyridyl]ethane (H_2BPG_2E). H_2BPG_2E forms μ-oxodiaquadiiron(III) complexes $[Fe_2(\mu\text{-}O)(H_2O)_2(BPG_2E)]X_2$ [X = ClO_4 (**2a**) or OTf (**2b**)] that efficiently catalyzes epoxidation of various alkenes with H_2O_2. Upon reaction of **2b** with H_2O_2, a new purple species was formed and isolated at low temperatures. The purple species was characterized spectroscopically.

EXPERIMENTS: Preparation and isolation of purple species. To a solution of **2b** (83.7 mg 83.7 μmol) in MeCN (1 mL) was added 2.0 equiv of Et_3N (120 mM) at -40°C. To the solution was added 500 equiv of H_2O_2 (10 M), and stirred for 5 min. The solution turned dark purple. To the solution was added 15 mL of Et_2O at -40°C, then purple solid precipitated. The supernatant was decanted off, and the precipitate was washed with Et_2O several times at -40 °C. The purple solid was dried in vacuo. The isolated solid is stable at low temperature, and not changed several days at room temperature under dark in the absence of organic compounds potentially acting as reductant. Yield 35.1 mg (60 %). Anal. Calcd for $C_{30}H_{46}N_6O_{15}Fe_2$: C, 42.77; H, 5.50; N, 9.98%. Found: C, 42.63; H, 4.90; N, 9.82%. The isolated solid was used for various spectral measurements including the Mössbauer spectra.

RESULTS: The zero-field Mössbauer spectra of the isolated solid were recorded at some different temperatures raised from 23 to 295 K, then recorded again using the same sample by recooling to 17 K as shown in Figure 1. The spectrum at 23 K mainly consists of two quadrupole doublets with δ = 0.481(2) mm/s, ΔE_Q = 1.657(2) mm/s and δ = 0.20(3), ΔE_Q = 0.40(6), as shown by the deconvolution spectra composed of components ***a*** (red spectrum) and ***b*** (blue spectrum) in Figure 1, respectively. The intensity ratio of ***a*** and ***b*** is almost 90 : 10 at 23 K. When the temperature was increased to 100, 200, 250, and 293 K the component ***a*** (red spectrum) was decreased with the increase of ***b*** (blue spectrum). The ratios of ***a*** : ***b*** estimated from the deconvolution spectra are 85 : 15, 76 : 24, 59 : 41, and 45 : 55 at 100, 200, 250, and 293 K, respectively. The δ and ΔE_Q values of ***a*** at 100 K, 0.392(4) and 1.650(2) mm/s, are close to 0.53-0.68 and 1.51-1.90 mm/s of peroxodiiron(III) intermediate P in sMMO[1] and their model compounds. Thus, component ***a*** may be assigned to μ-oxo-μ-peroxodiiron(III) **3** with a symmetric structure. The δ and ΔE_Q values of the component ***b*** at 24-293 K, 0.131(3)-0.26(2) and 0.40(6)-0.55(3) mm/s, are almost in the range of δ = 0.14-0.21 and ΔE_Q = 0.53-0.68 mm/s of high-spin oxodiiron(IV) in the intermediate Q of sMMO.[1] High-spin (S = 2) oxoiron(IV) complexes reported so far show the δ and ΔE_Q values around 0.1 and 0.5 mm/s, respectively,[15] but low-spin (S = 1) oxoiron(IV) complexes have relatively higher ΔE_Q values of 1-2 mm/s.[21] Thus, component ***b*** may be assigned to high-spin oxodiiron(IV) similar to the intermediate Q and the synthetic high-spin oxoiron(IV) complexes. In conclusion, ***a*** and ***b*** are assigned to μ-oxo-μ-peroxodiiron(III) **3** and high-spin μ-oxodioxodiiron(IV) **4**, respectively.

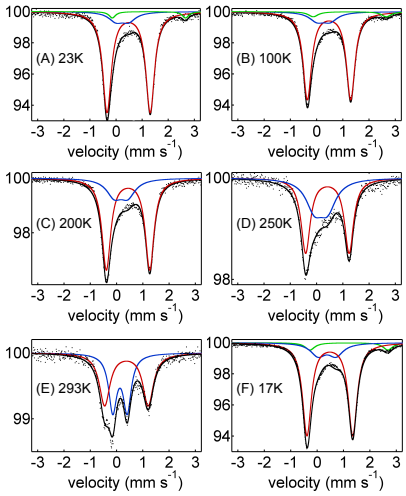

Fig 1. Zero field Mössbauer spectra of the isolated solid, recorded by raising the temperatures at (A) 23, (B) 100, (C) 200, (D) 250, and (E) 293 K, and by recooling the same sample at (F) 17 K. The black line is the least-square fitting to the raw data, and the red (component ***a***), blue (component ***b***), and green (component ***c***) lines are the deconvolution spectra corresponding to μ-oxo-μ-peroxodiiron(III) **3**, μ-oxodioxodiiron(IV) **4**, and diiron(II) complexes.

REFERENCES:

[1] (a) L. Shu, J. C. Nesheim, K. Kauffmann, E. Münck, J. D. Lipscomb, L. Que, Science, **275** (1997) 515; (b) C. E. Tinberg, S. J. Lippard, Acc. Chem. Res., **44** (2011) 280.
[2] M. Kodera, M. Itoh, K. Kano, T. Funabiki, M. Reglier, Angew. Chem. Int. Ed., **44** (2005) 7104.
[3] M. Kodera, Y. Kawahara, Y. Hitomi, T. Nomura, T. Ogura, Y. Kobayashi, J. Am. Chem. Soc., **134** (2012) 13236.

採択課題番号25082　　パーオキソニ核鉄(Ⅲ)とトリオキソニ核鉄(Ⅳ)の相互変換に関するメスバウアースペクトルによる研究　　共同通常

（同大院理）小寺政人、河原由佳　（京大・原子炉）北尾真司、瀬戸　誠

CO12-11 Test of a Microcell Multi-Wire Proportional Chamber for a Muon-Electron Conversion Experiment, DeeMe

H. Natori, N. Abe[1], M. Aoki[2], Y. Igarashi, S. Ito[2], S. Mihara, T. D. Nguyen[2], T. M. Nguyen[2], H. Nishiguchi, Y. Seiya[3], K. Shimizu[3], T. Takahashi[1] and K. Yamamoto[3]

High Energy Accelerator Research Organization (KEK)
[1] Research Reactor Institute, Kyoto University
[2] Department of Physics, Osaka University
[3] Department of Physics, Osaka City University

INTRODUCTION: DeeMe project [1] is an experiment to be conducted from 2015 at J-PARC Material and Life Science Experimental Facility (MLF) to search for a mu-e conversion, which is expected as a clear evidence of new physics. Detector is required to measure electron momentum precisely soon after a prompt burst particles, whose width and instantaneous hit rate is expected to be approximately 200ns and 20GHz/mm^2. We have been developing a micro-cell multi-wire proportional chamber (MWPC) for this project. In this experiment, we examined high rate tolerance using a prototype of the MWPC.

EXPERIMENTS: Experimental setup is shown schematically in Fig. 1. Electron beam collimated to 16mm × 19mm penetrates MWPC and beam counters. Beam rate is tuned changing current of electron gun heater.

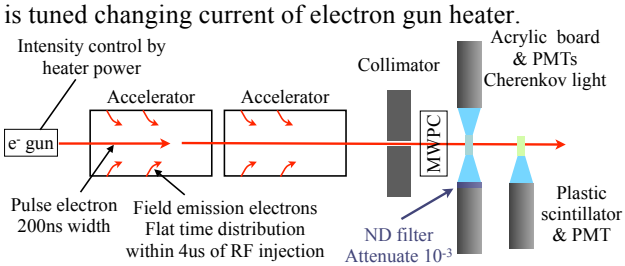

Fig. 1. Schematics of experimental setup. Electron momentum, beam width and repetition rate are set to be 30MeV/c, 200ns and 30Hz respectively.

Beam counters measure electron beam rate covering a rage from 1 to 10^7 electrons per pulse. One photomultiplier tube (PMT) connected to a plastic scintillator counts the number of electrons from 1 to a few hundreds. Middle range is covered using Cherenkov light, whose yield is smaller than scintillator, and high range using ND filter with light attenuation of 10^{-3}. At first, Electron gun is turned off to measure single electron utilizing field emission electrons. Then beam gun is turned on, gradually increasing beam rate. Main pulse and field emission electrons emulate prompt burst particles and delayed electrons respectively.

RESULTS: Field emission electrons are observed soon after a burst pulse when its instantaneous hit rate is approximately 50 MHz/mm^2 as shown in Fig. 2.

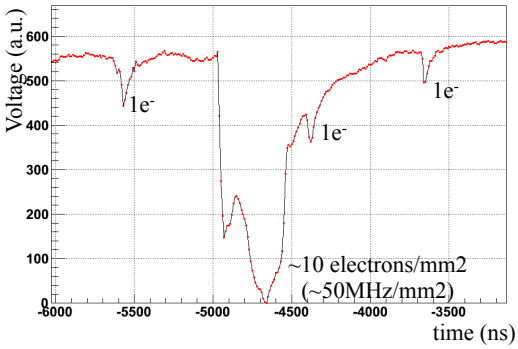

Fig. 2. MWPC waveform. Main pulse corresponds to approximately 50MHz/mm^2 in instantaneous hit rate. Three field emission electrons are observed

With increased beam rate, the prototype MWPC survived without any trip, but amplifiers are saturated and field emission electron was not observable. Fig. 3 shows raw waveforms of MWPC without amplifiers. We observed a gain drop by a space charge effect from beam rate of a few GHz/mm^2. Based on this result, we are developing a new technique to solve the problem. We are going to test the new technique in the coming beam test.

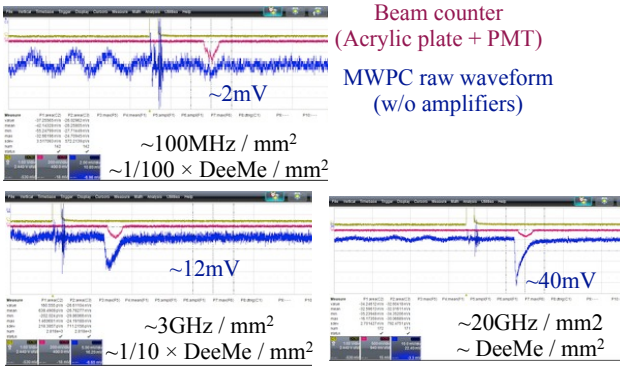

Fig. 3. MWPC raw waveform with different beam rate. Beam counter waveform represents beam structure. MWPC waveform is distorted from a few GHz/mm^2 due to gain drop by a space charge effect.

REFERENCES:

[1] M. Aoki and DeeMe Collaboration, AIP Conf. Proc. **1441** (2012) 599-601.

採択課題番号 25119　　ミューオン・電子転換過程探索実験 DeeMe 用プロトタイプ極小セル型チェンバーのビーム試験　　共同即時

（KEK）名取寛顕、五十嵐洋一、西口 創、三原 智（京大・原子炉）阿部尚也、高橋俊晴（阪大・理）青木正治、伊藤慎太郎、N. D. Thong、N. M. Truong（大阪市大・理）清水宏祐、清矢良浩、山本和弘

CO12-12

Development of Wide Dynamic Range Neutron Flux Monitor Having Fast Time Response

M. Isobe, K. Ogawa, H. Miyake[1], T. Kobuchi[1], H. Hayashi[1], Y. Nakano[2], K. Watanabe[2], A. Uritani[2] and T. Misawa[3]

Department of Helical Plasma Research, NIFS
[1]Department of Engineering Technical Services, NIFS
[2]Department of Materials, Physics and Engineering, Nagoya University
[3]Research Reactor Institute, Kyoto University

INTRODUCTION: The Large Helical Device (LHD), based at the National Institute for Fusion Science (NIFS), is the largest superconducting heliotron-type magnetic confinement system, providing an excellent opportunity to study three-dimensional currentless plasmas [1]. So far, high β value, high ion and electron temperatures, and long pulse operation capabilities in hydrogen discharges have been demonstrated. To explore higher-performance plasmas, the LHD project will step into a new stage, i.e., deuterium experiments. To execute this project as scheduled steadily and safely, a fast response, wide dynamic range neutron flux monitor (NFM) is essentially required in terms of both plasma physics and radiation safety. In TFTR and JT-60U tokamaks, a wide dynamic range NFM had been employed [2,3]. The electronics used in the two tokamaks were based on traditional analog circuits and is no longer commercially available at this moment. Therefore, we have been developing the wide dynamic range NFM optimized for LHD by using leading-edge digital signal processing (DSP) technologies.

EXPERIMENTS: In this work, we tested the prototype of DSP in Kyoto University Critical Assembly (KUCA) in 2013 to check its usability and performance of the unit. The unit has both functions of pulse counting and Campbelling (or MSV) modes. In particular, continuity from the pulse counting mode to the Campbelling mode was of great concern because the NFM system will work in the pulse counting mode whereas it will be mainly operated in the Campbelling mode in actual deuterium-beam-heated LHD discharges. As for a neutron detector, a ^{235}U fission chamber loaned from the KUCA facility, WL-8073 of Westinghouse Electric Co., was employed. The fission chamber was inserted into the B-reactor and thermal neutron fluxes up to ~10^7 (cm^{-2}•s^{-1}) were irradiated. The configuration is shown in Fig. 1. The Campbelling mode consists of three different schemes in its gain, i.e., H-gain, M-gain, and L-gain. In this experiment, a test of the Campbelling mode up to M-gain could be managed.

RESULTS: Numbers of output pulses indicated by our system were proportional to those of the fission chamber and the uncompensated ion chamber (UIC) of the KUCA, and γ-ray ionization monitor placed on the reactor hall wall. As an example, a result of comparison in time evolution of signal outputs between our system and the KUCA UIC is shown in Fig. 2. Good agreement can be recognized between the two in time trend. An unwanted sharp peak is seen in our signal. Judging from detailed analysis on the three different Campbelling mode signals, the sharp peak is not due to failure of our system, and is rather due to noise. It should be noted that this issue can be overcome by employing robust electromagnetic shield. In summary, a satisfactory prospect was obtained toward manufacture of actual DSP unit for the NFM on the LHD through preliminary operation test in the KUCA.

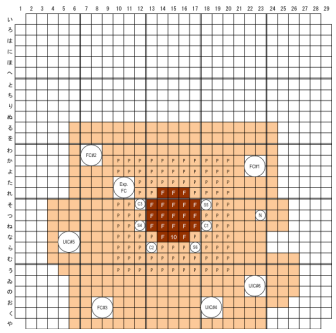

Fig. 1. Arrangement of ^{235}U fission camber, designated as Exp. FC in the B-reactor of KUCA.

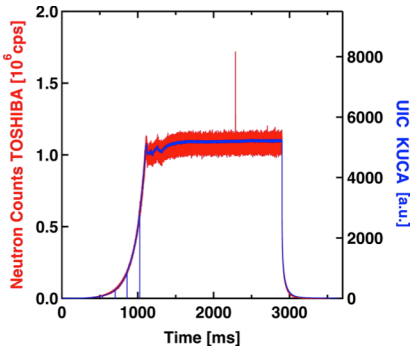

Fig. 2. Comparison of time evolution of output signals between the NIFS/TOSHIBA-NFM equipped the DSP prototype and the UIC of KUCA.

REFERENCES:

[1] O. Kaneko *et al.*, Nucl. Fusion **53** (2013) 104015.
[2] A.C. England *et al.*, Rev. Sci. Instrum. **57** (1986) 1754.
[3] T. Nishitani, J. Japan Soc. of Plasma Sci. and Nucl. Fus. Res. **68** (1992) 6. (in Japanese)

採択課題番号 CA25107　デジタル信号処理を利用した広いダイナミックレンジと高速応答特性を持つ中性子フラックスモニタの検討　共同通常

（核融合研・研究部）磯部光孝、小川国大、（核融合研・技術部）三宅　均、小渕　隆、林　浩
（名大・工）仲野裕次、渡辺賢一、瓜谷章、（京大・原子炉）三澤　毅